Three-Dimensional Kinematics of Ocular Drift in Humans With Cerebellar Atrophy

D. STRAUMANN,[1,2] D. S. ZEE,[1,3] AND D. SOLOMON[1]
[1]*Department of Neurology, Johns Hopkins Hospital, Baltimore 21287;* [2]*Department of Neurology, Zurich University Hospital, CH-8091 Zurich, Switzerland; and* [3]*Departments of Ophthalmology and Otolaryngology—Head and Neck Surgery, Johns Hopkins Hospital, Baltimore, Maryland 21287*

Straumann, D., D. S. Zee, and D. Solomon Three-dimensional kinematics of ocular drift in humans with cerebellar atrophy. *J. Neurophysiol.* 83: 1125–1140, 2000. One of the signs of the cerebellar ocular motor syndrome is the inability to maintain horizontal and vertical fixation. Typically, in the presence of cerebellar atrophy, the eyes show horizontal gaze-evoked and vertical downbeat nystagmus. We investigated whether or not the cerebellar ocular motor syndrome also includes a torsional drift and, specifically, if it is independent from the drift in the horizontal-vertical plane. The existence of such a torsional drift would suggest that the cerebellum is critically involved in maintaining the eyes in Listing's plane. Eighteen patients with cerebellar atrophy (diagnosis confirmed by magnetic resonance imaging) were tested and compared with a group of normal subjects. Three-dimensional eye movements (horizontal, vertical, and torsional) during attempted fixations of targets at different horizontal and vertical eccentricities were recorded by dual search coils in a three-field magnetic frame. The overall ocular drift was composed of an upward drift that increased during lateral gaze, a horizontal centripetal drift that appeared during lateral gaze, and a torsional drift that depended on horizontal eye position. The vertical drift consisted of two subcomponents: a vertical gaze-evoked drift and a constant vertical velocity bias. The increase of upward drift velocity with eccentric horizontal gaze was caused by an increase of the vertical velocity bias; this component did not comply with Listing's law. The horizontal-eye-position–dependent torsional drift was intorsional in abduction and extorsional in adduction, which led to an additional violation of Listing's law. The existence of torsional drift that is eye-position–dependent suggests that the cerebellum is critically involved in the implementation of Listing's law, perhaps by mapping a tonic torsional signal that depends on the direction of the line of sight. The magnitude of this signal might reflect the difference in torsional eye position between the torsional resting position determined by the mechanics of the eye plant and the torsional position required by Listing's law.

INTRODUCTION

In normal human subjects, eye positions during steady fixation follow a mathematical specification named Listing's law: if ocular positions during fixation are expressed as single rotations from a common reference position, all rotation axes lie in a plane, the so-called Listing's plane (Helmholtz 1867). Hence, Listing's law seems to be a fundamental property of the ocular fixation system. To a lesser degree, Listing's law also applies to smooth pursuit eye movements and saccades (Haslwanter et al. 1991; Straumann et al. 1996; Tweed and Vilis 1990; Tweed et al. 1992). Listing's law also specifies Donders' law, which states that ocular torsion is unique for every direction of gaze (Donders 1848).

A fundamental question of ocular motor physiology is whether or not pathological eye movements can be identified that do not comply with Listing's law, and if these eye movements can be related to specific lesions in premotor, motor, or peripheral structures of the ocular motor system (Straumann and Zee 1995). Theoretically, four types of violations of Listing's law can be expected: I, scattering of three-dimensional eye positions on a nonplanar surface during fixations and movements; II, transient deviations from Listing's plane during and after changes in eye position; III, active torsional movements out of Listing's plane; and IV, passive torsional drift movements out of Listing's plane.

Type I violations of Listing's law can be caused by mechanical alterations of the ocular plant, e.g., orbital tumors.

Type II violations are transient and occur if, during a movement, the axis of angular velocity does not tilt in the direction of gaze by a geometrically specified angle to compensate for the noncommutativity of rotations (the so-called half-angle rule). To a small degree, such torsional blips (peak torsional deviations $\leq 2°$) can be seen during and after normal saccades (Straumann et al. 1995, 1996). Large torsional blips called macroblips (peak torsional deviations $\sim 10°$) were described in a patient with a lesion involving the cerebellar vermis, its deep nuclei, and the dorsolateral medulla, suggesting that the cerebellum might be involved in implementing Listing's law (Helmchen et al. 1997).

Type III violations of Listing's law are to be expected because any active torsional movement corresponds to such a violation. They generally occur during vestibular stimulation both normally, e.g., during torsional vestibular nystagmus (Crawford and Vilis 1991), and in disease, e.g., during vertical-torsional benign paroxysmal positioning nystagmus (Fetter and Sievering 1995).

Type IV violations of Listing's law are still hypothetical. They would reflect the failure of the CNS to maintain the eyes in Listing's plane. Recent models of the three-dimensional velocity-to-position integrator assume that, in the absence of vestibular stimulation, only the horizontal and vertical components of the velocity-to-position integrator are being loaded, which implicitly results in eye positions in Listing's plane (Quaia and Optican 1998; Schnabolk and Raphan 1994; Tweed and Vilis 1987). In other words, velocity signals from the saccadic and the pursuit systems are such that their integration

The costs of publication of this article were defrayed in part by the payment of page charges. The article must therefore be hereby marked "*advertisement*" in accordance with 18 U.S.C. Section 1734 solely to indicate this fact.

does not lead to a change in torsional eye position, which should always be zero if Listing's law is valid and three-dimensional eye position is encoded in a coordinate system that is equivalent to rotation or quaternion vectors. It is important to realize that this view implies that the ocular plant is constructed such that, in the absence of an eye-position–dependent torsional tonic signal, Listing's law is automatically implemented. In this case, leaky velocity-to-position integration in the presence of saccadic or pursuit velocity signals will always lead to drift movements exclusively in Listing's plane. If, however, the mechanics of the eye plant do *not* implement Listing's law for fixations, it is necessary that the ocular motor system produce a tonic torsional signal that is specified by the horizontal and vertical gaze direction. This tonic torsional signal must compensate the torsional error caused by the "non-Listing mechanics" of the ocular globe. It follows that a failure to map correctly the appropriate tonic torsional signal to the horizontal-vertical direction of gaze will lead to an eye movement drifting out of Listing's plane after each saccade. The amplitude of this slow torsional eye movement, in the absence of an intervening saccade, would vary with gaze direction.

It is likely that the elastic extorsional and intorsional forces acting on the ocular globe do not perfectly cancel for any direction of gaze. For instance, Seidman et al. (1995) were able to show that the time constants of torsional drift, after mechanically forcing the eyes to extorsional or intorsional offset positions, are different. Assuming such an anisotropy of elastic restoring forces in the torsional direction, tonic torsional signals become indispensable to maintain the eye in Listing's plane during fixations. Moreover, it may be that the ocular motor system holds two separate Listing's planes: one determined by the mechanical configuration of the eye plant, the other implemented by the CNS. If the orientation of the "mechanical Listing's plane" were different from the "neural Listing's plane," the absence of tonic torsional signal would lead to a drift from "central" to "mechanical" Listing's positions.

Examining patients with a cerebellar ocular motor syndrome, in which it is difficult to maintain fixation, is a good way to test if type IV violations of Listing's law exist. Typically, the eyes drift both upward and in the horizontal-centripetal direction, which results in downbeat and horizontal gaze-evoked nystagmus, respectively (Leigh and Zee 1999). We attempted to determine whether or not patients with cerebellar atrophy also have abnormal torsional drift movements and, by that, demonstrate the existence of a type IV violation of Listing's law. The following specific questions were asked: is Listing's law valid in patients with cerebellar atrophy? Is the ocular drift in these patients two-dimensional (horizontal and vertical) or three-dimensional (horizontal, vertical, and torsional)? If present, is the torsional drift independent of the drift in the vertical or horizontal direction?

We show that, in addition to the well-known horizontal gaze-evoked and upward drifts, there is a drift in the torsional direction that is dependent on the horizontal eye position. This torsional drift is independent of the upward drift and its velocity does not correlate with the velocity of horizontal drift. Thus the data suggest that the cerebellum is involved in mapping an appropriate tonic torsional signal for every direction of the line of sight.

METHODS

Subjects

Eighteen patients (P1-P18, age 40–69 yr, 9 female) with horizontal gaze-evoked and downbeat nystagmus associated with cerebellar atrophy, as demonstrated by magnetic resonance imaging, were studied. The cerebellum was diffusely atrophied in each patient, i.e., both the paramedian and hemispheric cerebellar structures were affected. None of the patients had neuroradiological or clinical findings that were suggestive of extracerebellar involvement. The ocular motor findings were typical for the syndrome of the flocculus/paraflocculus (impaired smooth pursuit system; postsaccadic drift; and gaze-evoked, downbeat, and rebound nystagmus). An additional deficiency of the nodulus, ventral uvula, dorsal vermis, or fastigial nuclei was likely, but no specific ocular motor tests were performed to assess the function of these structures.

Fourteen patients were tested at the Johns Hopkins Hospital in Baltimore, Maryland, and four patients were tested at Zurich University Hospital, Switzerland. The comparison group consisted of 25 normal subjects (N1-N25, age 18–54 yr, 16 female), 21 of which were tested in Baltimore, the others in Zurich. The visual acuities in the normal subjects were 20/20 corrected. In Baltimore, informed written consent from patients and normal subjects was obtained after an explanation of the experimental procedure, which was in accordance with the standards of and was approved by the Johns Hopkins Joint Committee on Clinical Investigation. In Zurich, the paradigms of this study were part of the standard ocular motor testing battery. At the time of patient recording, unwritten informed consent was sufficient.

Experimental setup

The experimental setups in Baltimore and Zurich were identical unless stated otherwise. Ocular rotation of both eyes around all three principal axes (torsional, roll, x axis; vertical, pitch, y axis; and horizontal, yaw, z axis) was simultaneously recorded with dual search coils (Skalar, Delft, Netherlands). The field coil system consisted of a cubic coil frame of welded aluminum that produced three orthogonal magnetic fields with frequencies of 55.5, 83.3, and 42.6 kHz and intensities of 0.088 gauss. Amplitude-modulated signals were extracted by synchronous detection. The bandwidth of the system was 0–90 Hz. Peak-to-peak noise signals in all three principal directions after calibration, as measured by a dual search coil placed in the center of the magnetic frame, were ~0.05° in Baltimore and ~0.1° in Zurich. The side length of the coil frame in Baltimore was 1.02 m, in Zurich 1.40 m.

Calibration procedure

The voltage offsets of the system were zeroed by placing the dual search coils in the center of a metal tube that shielded them from the magnetic fields. Thereafter, the relative gains of the three magnetic fields were determined with the search coils on a gimbal system in the center of the coil frame. The details of the calibration procedure and the computation of three-dimensional eye position are given in Straumann et al. (1995).

The three-dimensional eye position in the coil frame was expressed in rotation vectors. A rotation vector $r = (r_x, r_y, r_z)$ describes the instantaneous orientation of a body as a single rotation from the reference position. The vector is oriented parallel to the axis of this rotation and its length is defined by $\tan(\rho/2)$, where ρ is the rotation angle. The coordinate system of rotation vectors was defined by the three head-fixed orthogonal axes of the coil frame with the x axis pointing forward, the y axis leftward, and the z axis upward. The signs of rotations around these cardinal axes were determined by the right-hand rule, i.e., clockwise, leftward, and downward rotations, as seen by the subject, were positive.

For each experimental trial, a plane was fitted through the data cloud of all rotation vectors:

$$r_x = a_0 + a_1 r_y + a_2 r_z$$

The offset a_0, the y slope a_1, and the z slope a_2, which determined the orientation of this best-fit plane, were used to rotate all eye positions such that this plane coincided with the y-z plane of the coordinate system, and therefore the primary position with the reference position $r_{\text{ref}} = (0, 0, 0)$. The corresponding vector r_{p} for this rotation was given by (Haustein 1989)

$$r_{\text{p}} = (-a_0, -a_1, a_2)$$

From the rotation vectors that were rotated as described above, three-dimensional angular velocity vectors ω were computed using the formula (Hepp 1990)

$$\omega = 2(dr + r \times dr)/(1 + |r|^2)$$

where dr denotes the derivative of r and $\times$ the cross product. Note that, because of the noncommutativity of rotations, three-dimensional angular velocity is not simply the derivative of position.

For convenience, the lengths of rotation and angular velocity vectors were given in degrees (°) and degrees per second (°/s), respectively, but the right-hand rule was maintained when describing the orientation of these vectors.

Experimental procedures

Subjects were seated inside the field coil so that the center of the interpupillary line coincided with the center of the frame. The head of the subject was immobilized with a bite bar that was oriented in an earth-horizontal plane with no rotation around the earth-vertical axis. Dual search coils were mounted on both eyes after the conjunctiva was anesthetized with proparacaine HCL 0.5% (Ophthetic).

During experiments, subjects were asked to fix on light-emitting diodes (LEDs) at different locations of an earth-vertical tangent screen that was positioned 1.24 m in front of the center of the eyes. LEDs were consecutively switched on and off such that only one LED was lit at any time in dim light or complete darkness. In Zurich, light dots were rear-projected onto a translucent tangent screen.

Voltages related to the orientation of the eye coils in the magnetic frame were digitized with a 12-bit A/D converter at 500 Hz and written to a hard disk. The data were analyzed off-line in MATLAB version 5.1.

Paradigms

The eight eccentric positions of the light dot used as the fixation stimulus were arranged on a square around the straight-ahead position. Four positions were situated ±20° from the center on the horizontal and vertical meridians, and four other positions were situated ±28.3° from the center on the two oblique meridians. Eccentric positions were consecutively lit in the counterclockwise direction. Before the appearance of each eccentric stimulus, the center position was lit so that subjects always made centrifugal and centripetal shifts of eye position. Each fixation period lasted 2.5 s. In one paradigm, the LED was on during the entire fixation period; in another paradigm, the LED was switched off after 0.5 s and switched on again for the last 0.5 s of the fixation period. Switching off the LED for some time during the fixation period did not have any effect on eye drift except that it was more difficult for the patients keep their eyes near the desired positions because of persistent centripetal and upward drift. In the analysis, we therefore used the data from the paradigms in which the LEDs were not intermittently switched off. Paradigms were repeated for binocular viewing and monocular viewing of either eye. In this study, only monocular data of the viewing eye are reported.

Torsional coil slippage

During search coil recordings, a long-term drift of torsional coil signals is frequently observed, which is most likely caused by a gradual slippage of the silicon annulus on the conjunctiva around the line of sight (Straumann et al. 1996; Van Rijn et al. 1994). Therefore the fixations that we used to determine Listing's plane were all inside a time interval of 60 s. When analyzing slow-phase eye movements of nystagmus at the angular velocity level, however, the very slow artificial change of torsional eye position signals was negligible because here we were interested in the three-dimensional angular drift direction of the eyes and not absolute ocular position. For this analysis, we used data from entire trials lasting 120 s, during which paradigms were performed three times by the subjects.

Pooling of binocular data

In 17 of the 18 patients, eye movement recordings from both eyes were available. In one patient, the signals of one eye were corrupted because the wires of the annulus broke during recording. Of the 25 healthy subjects, 20 were measured with annuli on one eye and the other five had annuli on both eyes. Tables and statistical values were based on pooled data whereby data from the left eyes were mirrored. For convenience, summary figures contain only data from right eyes, but statistical information in the text is based on pooled data.

RESULTS

Listing's law

We attempted to determine if Listing's law is obeyed in patients with cerebellar atrophy. Because these patients showed spontaneous nystagmus, especially downbeat nystagmus and horizontal gaze-evoked nystagmus, it was not a priori evident during which phase of a nystagmus cycle eye positions should be selected to test the validity of Listing's law. We chose to perform the analysis for four different data subsets extracted from single experimental trials: *1*) all eye positions, *2*) desaccaded eye positions (fixations and slow phases), *3*) presaccadic eye positions (interval of 5–55 ms before the beginning of quick phases), and *4*) postsaccadic eye positions (interval of 5–55 ms after the end of the quick phases).

Figure 1 demonstrates examples of single experimental trials. Eye positions are plotted as rotation vectors in the front (*top row*, *y*-*z* plane), side (*middle row*, *x*-*z* plane), and top (*bottom row*, *x*-*y* plane) views of the coordinate system. Trials consisted of 2–3 cycles. For this figure and for the entire analysis presented in this subsection, *Listing's law*, only single cycles of trials were selected. Such a restriction of the time interval was chosen because long-term torsional drifts of scleral annuli can lead to artificial "thickening" of Listing's plane (see METHODS).

Figure 1, *A* and *B*, shows ocular rotation vectors of a cerebellar patient (P8, right eye) in different views. Whereas the Cartesian coordinate system in Fig. 1*A* is determined by the magnetic coil frame, the data in Fig. 1*B* are rotated such that the best-fit plane through the data cloud aligns with the *y*-*z* plane of the coordinate system (see METHODS). For comparison, Fig. 1*C* depicts rotated ocular rotation vectors (right eye) of a normal subject (N7).

Clearly, the cerebellar patient was not able to maintain fixation (Fig. 1, *A* and *B*). During attempted fixation along positions with no horizontal eccentricity, trajectories were oriented parallel to the *y* axis, which corresponded to the observed

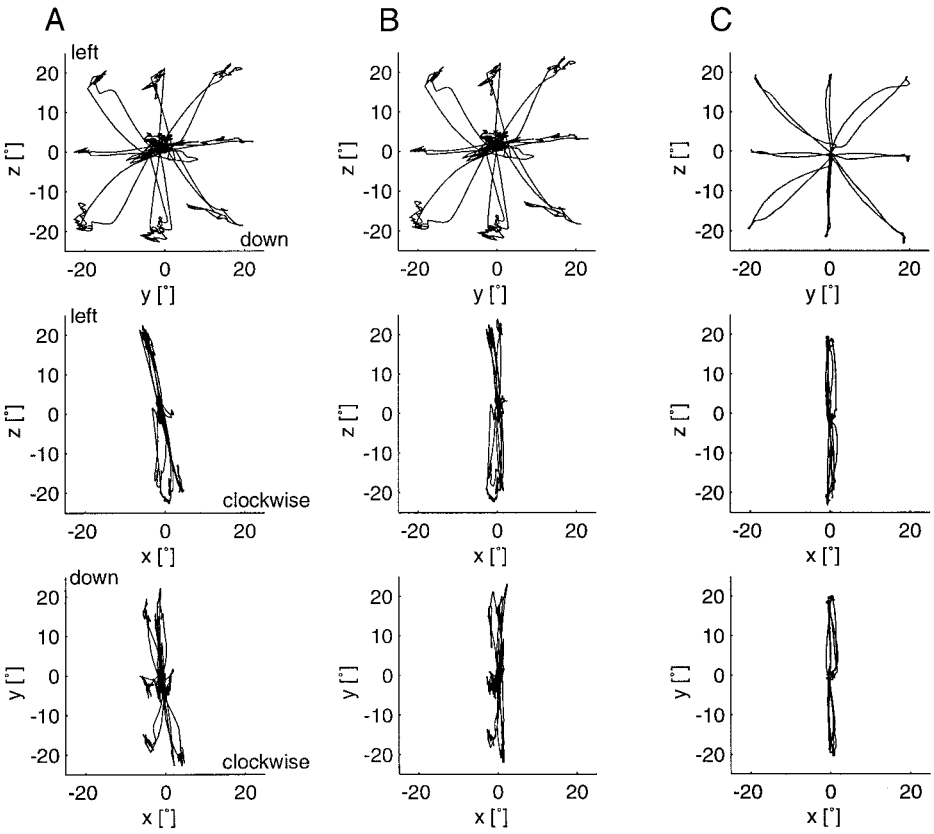

FIG. 1. Examples of three single trials. Attempted fixations of a central and eight eccentric targets on a tangent screen. *x*, torsional; *y*, vertical; *z*, horizontal components of rotation vectors in °. Signs of base vector directions according to the right-hand rule. *Top*: front view (*y*-*z* plane). *Middle*: side view (*x*-*z* plane). *Bottom*: top view (*x*-*y* plane). *A*: patient P8, right eye, unrotated data (zero vector is straight ahead). *B*: rotated data of *A* (zero vector is primary position). SD of first-order linear fit: 1.09°; SD of second-order linear fit: 0.55°; twist score: 0.454. *C*: rotated data of normal subject N7, right eye. SD of first-order linear fit: 0.53°; SD of second-order linear fit: 0.45°; twist score: 0.154.

downbeat nystagmus. If the eyes were moved to positions with a horizontal eccentricity, there was an additional horizontal gaze-evoked nystagmus and, therefore, drift trajectories were oblique (Fig. 1, *A* and *B*, *top*). After rotation of the patient's data from the coordinate system defined by the coil frame (Fig. 1*A*) to the Listing's coordinate system (Fig. 1*B*), it became evident (*middle* and *bottom*) that the width of Listing's plane in the patient was larger than that in the normal subject (Fig. 1*C*). This can be seen in both the *x*-*z* (*middle row*) and *x*-*y* (*bottom row*) projections.

The standard deviations of eye positions from the best-fit plane are summarized in Table 1 (pooled data from both eyes). This so-called thickness of Listing's plane (as reflected in the mean values of the standard deviations) was significantly higher in the group of 18 patients than in the group of 25 control subjects. (Throughout the entire paper, "significant" = $P < 0.05$). This was the case for all four data subsets. The differences between the patients and the control group, however, were small (0.17–0.20°). The average standard deviation of data points from the plane was almost the same for pre- and postsaccadic eye positions in patients and normal subjects. Note that the slopes (*y* and *z*) of the planar fits, which are related to the primary direction, were not significantly different between the two groups, e.g., for planes fitted to presaccadic fixations, the average *y* slope of pooled eyes (left eyes mirrored) was 0.01 ± 0.09 SD ($n = 35$) in the cerebellar patients and 0.01 ± 0.07 SD ($n = 30$) in the normal subjects. Corresponding average *z* slopes were −0.09 ± 0.09 SD and −0.08 ± 0.07 SD, respectively.

Data clouds of ocular rotation vectors were also fitted with linear second-order regressions of the form

$$r_x = a_0 + a_1 r_y + a_2 r_z + a_3 r_y^2 + a_4 r_y r_z + a_5 r_z^2$$

where a_3 and a_5 are measures for the curvature along the *y* and *z* axes and a_4 indicates how much the surface is twisted (Hore et al. 1992). Again, in all four subsets of data, patients differed significantly from normal subjects (Table 2). This means that the larger thickness of Listing's plane (= standard deviation

TABLE 1. *Standard deviations (in degrees) from first-order linear fits through eye rotation vectors during attempted fixation trials in patients and normal subjects*

	18 Patients (35 eyes)	25 Controls (30 eyes)	*P* (*t*-test)
All eye positions	0.95 ± 0.37 (0.82)	0.75 ± 0.22 (0.77)	0.004
Slow phases and fixations	0.89 ± 0.35 (0.82)	0.72 ± 0.22 (0.74)	0.010
Presaccadic eye positions	0.94 ± 0.36 (0.83)	0.75 ± 0.22 (0.73)	0.004
Postsaccadic eye positions	0.94 ± 0.37 (0.83)	0.75 ± 0.22 (0.73)	0.005

Values are means ± SD with the median in parentheses.

TABLE 2. *Standard deviations (in degrees) from second-order linear fits through eye rotation vectors during fixation trials in patients and normal subjects*

	18 Patients (35 eyes)	25 Controls (30 eyes)	*P* (*t*-test)
All eye positions	0.83 ± 0.35 (0.69)	0.63 ± 0.18 (0.64)	0.003
Slow phases and fixations	0.77 ± 0.32 (0.68)	0.61 ± 0.19 (0.61)	0.008
Presaccadic eye positions	0.81 ± 0.33 (0.73)	0.64 ± 0.19 (0.61)	0.005
Postsaccadic eye positions	0.82 ± 0.34 (0.71)	0.65 ± 0.18 (0.65)	0.007

Values are means ± SD with the median in parentheses.

from the planar fit) in the cerebellar patients was not caused by curving or twisting of the surface, on which three-dimensional eye positions lie, because otherwise the standard deviations of eye positions from the second-order fit would not be different in patients and normal subjects.

To confirm further that the increased thickness of Listing's plane in the patients was not caused by an increased twisting of Listing's surface, we computed the so-called twist factor *s*:

$$s = r_x / r_y r_z$$

In none of the four data subsets were twist factors significantly different in patients and normal subjects, e.g., the average twist factor for presaccadic fixations was 0.33 ± 0.33 SD in the patients and 0.42 ± 0.34 SD in the normal subjects ($P = 0.137$).

In summary, analysis of three-dimensional eye movements based on the positions of the eye revealed that Listing's law was less valid in the cerebellar patients than in the control group. Yet the differences in plane or surface thickness (standard deviations from best-fit first- or second-order linear fits) were small between the two groups. One explanation for this relatively small increase may be that quick phases effectively compensate for drift movements that do not comply with Listing's (and Donders') law (Lee et al. 1998; Van Opstal et al. 1996). This hypothesis is supported by the fact that the correlation between the thickness of Listing's plane and the drift velocity at 20° horizontal eccentricities (combined mean velocity in abduction and adduction) was weak ($R = 0.36$; $P = 0.029$; $n = 18$ right eyes + 17 left eyes) and that there was no significant correlation between the thickness of Listing's plane and the time constants of horizontal ($R < 0.01$, $P = 0.857$) or vertical ($R = 0.32$, $P = 0.057$) ocular drift (scatter plots not shown). At this point of analysis, however, we could not conclude that the drift movements in cerebellar patients violated Listing's law because, in the cerebellar patients, the eyes were constantly moving and it was therefore impossible to determine the "true" Listing's plane. As a result, we also could not determine in which period(s) of nystagmus the deviations from Listing's plane occurred or at which moment of the nystagmus cycle they were corrected.

To decide whether or not the drift movements complied with Listing's law, trajectories had to be analyzed at the angular velocity level. It follows from the definition of an angular velocity vector (see METHODS) that Listing's law specifies the value of the torsional vector component (ω_x) by an equation that includes the values of the two other components (ω_y and ω_z) and the vertical (r_y) and horizontal (r_z) components of the instantaneous rotation vector (Van den Berg 1995):

$$\omega_x = r_y \cdot \omega_z - r_z \cdot \omega_y$$

Solving this equation for a particular angular velocity vector that moves orthogonal to a radial line passing through the reference position, the angular velocity axis tilts out of Listing's plane by half the gaze angle in the direction of gaze. Accordingly, the equation is also know as the "half-angle rule."

In *Three-dimensional angular drift*, we present each of the three angular velocity components (vertical, horizontal, and torsional) of ocular drift separately. Then we correlate the drift components to see if they are independent from each other. Finally we attempt to determine if the ocular drift in the patients follows the half-angle rule, i.e., complies with Listing's law.

Three-dimensional angular drift

Figure 2 depicts an example of how the data were further processed. The vertical rotation vector component r_y of the same data shown in Fig. 1*B* is plotted as a function of time (*top*). Recall that the set of rotation vectors was rotated such that the best-fit plane through the data cloud aligned with the

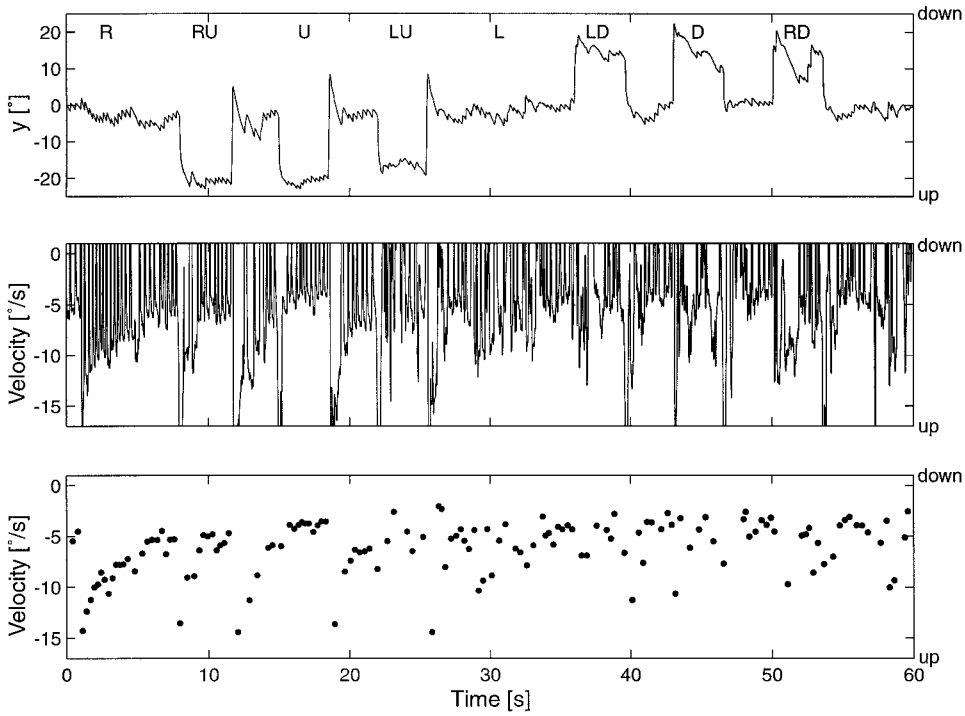

FIG. 2. Same data as in Fig. 1*B* (rotated data, patient P8, right eye), but only the vertical eye movement component is plotted as a function of time. *Top*: vertical rotation vector component. Letters indicate directions of attempted eccentric fixations after central fixation. R, right; RU, right-up; U, up; LU, left-up; L, left; LD, left-down; D, down; RD, right-down. *Middle*: vertical angular velocity vector component. *Bottom*: median vertical angular velocity component for each nystagmus slow phase.

y-z plane of the coordinate system. The letters above the eye position trace indicate which of the eight eccentric target lights was switched on to be fixed by the subject (R, right; RU, right-up; L, left; etc.). As described in *Paradigms*, subjects always had to look at the central target between eccentric fixations. In this example, there was a persistent drift of the eye in the upward (negative vertical) direction with compensatory downbeating quick phases.

Fig. 2, *middle*, contains the vertical component of the angular velocity vectors. Note that we always computed the angular velocity vectors from those rotation vectors that were rotated into the *y-z* plane, as described in *Calibration procedure*, because a tilt of Listing's plane with respect to the *y-z* plane of the coordinate system would introduce a "false reference-position–dependent torsion" (Suzuki et al. 1994).

For each slow phase of nystagmus, the median values of the horizontal, vertical, and torsional angular velocity components were computed. The corresponding vertical medians in the example are plotted in Fig. 2, *bottom*. The medians of the corresponding eye rotation vectors during each slow phase were also determined (not shown) so that each data point representing one slow phase consisted of three rotation and three angular velocity vector components. The data points were then assigned to one of the eight targets of attempted eccentric fixation. After selecting subsets of data according to the horizontal and vertical eye positions, components of rotation and angular velocity vectors were plotted against each other.

Each component of three-dimensional eye movements was specifically tested for the validity of Alexander's law (Alexander 1912; Robinson et al. 1984). This law describes the relation between the slow-phase eye velocity and the change in eye position along the velocity vector: as the eye moves in the direction of the slow phase, slow-phase velocity decreases. If the relation between eye position (independent variable) and eye velocity (dependent variable) forms a line, the negative slope is reciprocal to the time constant of the "velocity-to-position integrator" (Hess et al. 1984; Robinson et al. 1984).

Figure 3 depicts two examples of the relation between vertical eye position component r_y and vertical angular velocity component ω_y. Only data with the eye in center-up and center-down positions are plotted. The regression line was computed by fitting the data to the equation

$$\omega_y = a + r_y b$$

The following procedure was used: first-order linear regressions were iterated ≤20 times. After each regression, the data subset of points that were farthest away from the best-fit line was discarded. If the initial number of data points was >100, 1% of data points was discarded after each regression; if the initial number of data points was <100, only one data point was discarded after each regression. The procedure was repeated until 20% of the data were excluded from the fit. The offset (a), slope (b), and significance (P) of the last regression were further analyzed. If $P < 0.05$ and the slope "eye position divided by velocity" was negative, Alexander's law was said to be valid. If the slope was positive but P was still significant, this relation was named "inverse Alexander's law." If P was not significant, Alexander's law and inverse Alexander's law were rejected.

Figure 3*A* shows traces from the same experimental trial as in Figs. 1 and 2 (patient P8, right eye), but now the data is derived from the entire length of the trial, i.e., the sequence of eight targets appeared three times. The data points are widely scattered along the ordinate, but the negative correlation between vertical angular velocity and vertical eye position is still significant ($P < 0.05$). Alexander's law is therefore valid in this example (values given in the legend of Fig. 3). In Fig. 3*B*, which gives another example (patient P6, right eye), the correlation is even better ($P < 0.001$). The offset of the regression line in Fig. 3*A* is more negative than in Fig. 3*B*. The offset values represent an additional drift velocity that is unexplained by Alexander's law and that could be, for example, of vestibular origin. The presence of this additional drift velocity leads to a shift of the intercept of the regression line through the eye position axis (abscissa).

In the subsequent analysis, we name the slopes and offsets of the first-order regression between eye position and eye velocity according to the directions of the two variables, e.g., the ω_x-r_y slope is the slope of the regression between torsional angular velocity (ω_x, ordinate) and vertical eye position (r_y, abscissa). *Vertical drift*, *Horizontal drift*, and *Torsional drift* summarize vertical, horizontal, and torsional angular eye drifts as a function of horizontal-vertical gaze directions, thus describing ω_y-r_y, ω_z-r_z, ω_x-r_y, and ω_x-r_z slopes and offsets of the eyes of the cerebellar patients. As already stated in METHODS, the figures

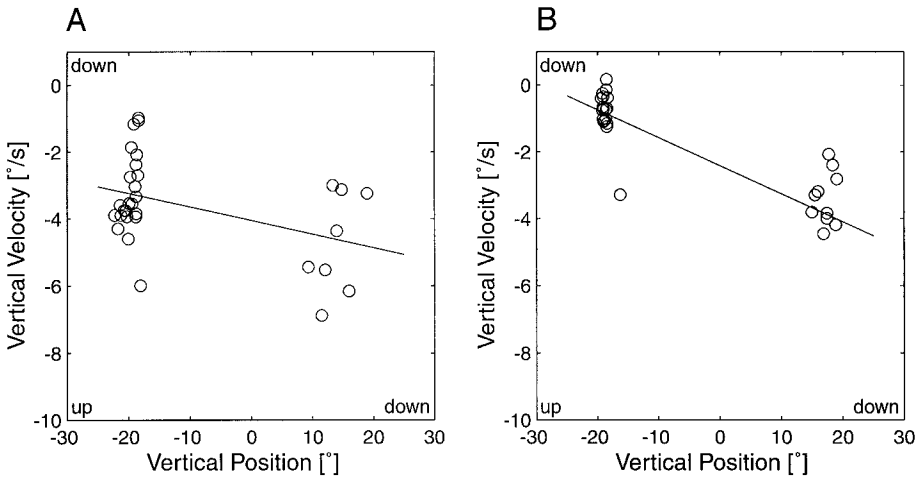

FIG. 3. Vertical angular velocity components of nystagmus slow phases as a function of gaze elevation during attempted fixations along the vertical meridian. First-order linear fits were computed by the fitting procedure described in *Three-dimensional angular drift*. *A*: patient P8, right eye (same trial as in Figs. 1 and 2); slope = −0.041, offset = −4.0, $P = 0.017$. *B*: patient P6, right eye; slope = −0.072, offset = −2.2, $P < 0.001$.

depict data from right eyes only, but in the text we present the data from both eyes.

Vertical drift

Figure 4*A* shows all ω_y-r_y slopes that were significant in the group of cerebellar patients (right eyes only). The first-order linear regressions were computed with gaze directed at three different horizontal target positions (center, 20° right, and 20° left). Dashed lines connect the data points of individual cerebellar patients. With gaze at zero horizontal eccentricity, 12 patients showed Alexander's law and six patients showed inverse Alexander's law (Fig. 4*A*, center data points). To visualize the differences in the ω_y-r_y slope caused by changing horizontal gaze direction, we subtracted the ω_y-r_y slope values for each subject obtained during fixations along the vertical meridian (Fig. 4*B*). No systematic change was observed as a function of horizontal eye position. For the pooled data ($n = 18$ right + 17 mirrored left eyes), the differences of ω_y-r_y slopes between the three horizontal gaze directions were not significant [*t*-tests: *P* (right-center) = 0.119; *P* (right-left) = 0.445; *P* (center-left) = 0.710].

For the ω_y-r_y offsets, the same two types of plots are shown in Fig. 4, *C* and *D*. Of the 18 patients, 15 showed negative ω_y-r_y offsets at zero horizontal gaze eccentricity, i.e., they had an upward drift when they attempted to look at the center target (Fig. 4*C*). There was a significant increase of ω_y-r_y offsets as patients moved their line of sight left or right (Fig. 4*D*). On average, this increase was similar both in adduction and abduction. For the pooled data, the differences of ω_y-r_y offsets between the two eccentric horizontal gaze directions and the central gaze direction were highly significant [*t*-tests: *P* (right-center) < 0.001; *P* (left-center) < 0.001], but the difference between the two eccentric positions was not significant [*t*-test: *P* (right-left) = 0.086].

Thus Fig. 4 demonstrates that the increase of downbeat nystagmus with horizontal gaze eccentricity is not caused by a further decrease of the time constant of the integrator, but is instead a result of an increased velocity bias and therefore independent of velocity-to-position integration. Note that in none of the patients was there a significant correlation between the ω_y-r_y offset (i.e., the vertical velocity bias) and the ω_y-r_y slope (i.e., the reciprocal of the vertical integrator time constant) for any of the three horizontal gaze directions.

Horizontal drift

The same steps of analysis used for vertical drift were also applied to horizontal drift. Figure 5, *A* and *B*, shows the ω_z-r_z slopes of the patients at three different vertical gaze eccentricities (20° up, center, and 20° down). Most data points were negative, consistent with Alexander's law (Fig. 5*A*). No differences were found between the ω_z-r_z slopes at different vertical eccentricities (Fig. 5*B*). This was confirmed for the pooled data [*t*-tests: *P* (up-center) = 0.076; *P* (up-down) = 0.575; *P* (center-down) = 0.129].

Velocity biases, i.e., ω_z-r_z offsets, were scattered around zero (Fig. 5*C*) with no tendency to shift in the positive or negative direction with changing vertical eccentricity (Fig. 5*D*). Indeed, for the pooled data, the differences between the three data sets were statistically not different [*t*-tests: *P* (up-center) = 0.269; *P* (up-down) = 0.380; *P* (center-down) = 0.970].

Thus Fig. 5 demonstrates that the time constant of the horizontal velocity-to-position integrator did not change when patients were looking up or down and that there was no

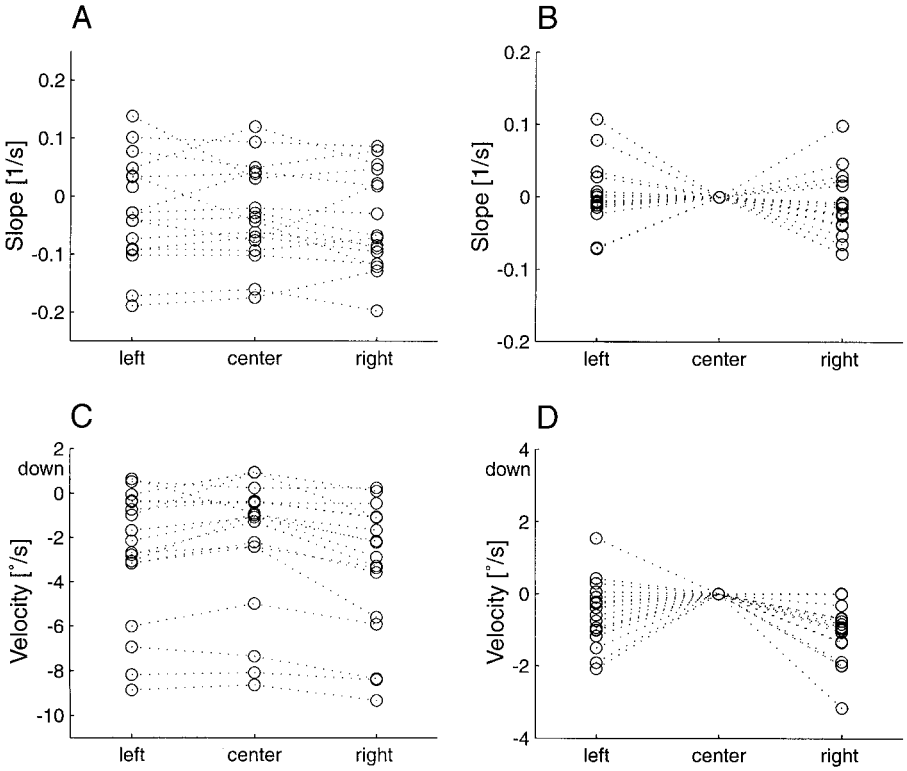

FIG. 4. Cerebellar patients, right eyes. Attempted fixations along vertical lines. Abscissa: 20, 0, −20° horizontal eccentricities. Data points of individual patients are connected by dashed lines. *A*: ω_y-r_y slopes of significant fits. *B*: differences of ω_y-r_y slopes from the values at 0° eccentricity. *C*: ω_y-r_y offsets. *D*: differences of ω_y-r_y offsets from the values at 0° eccentricity.

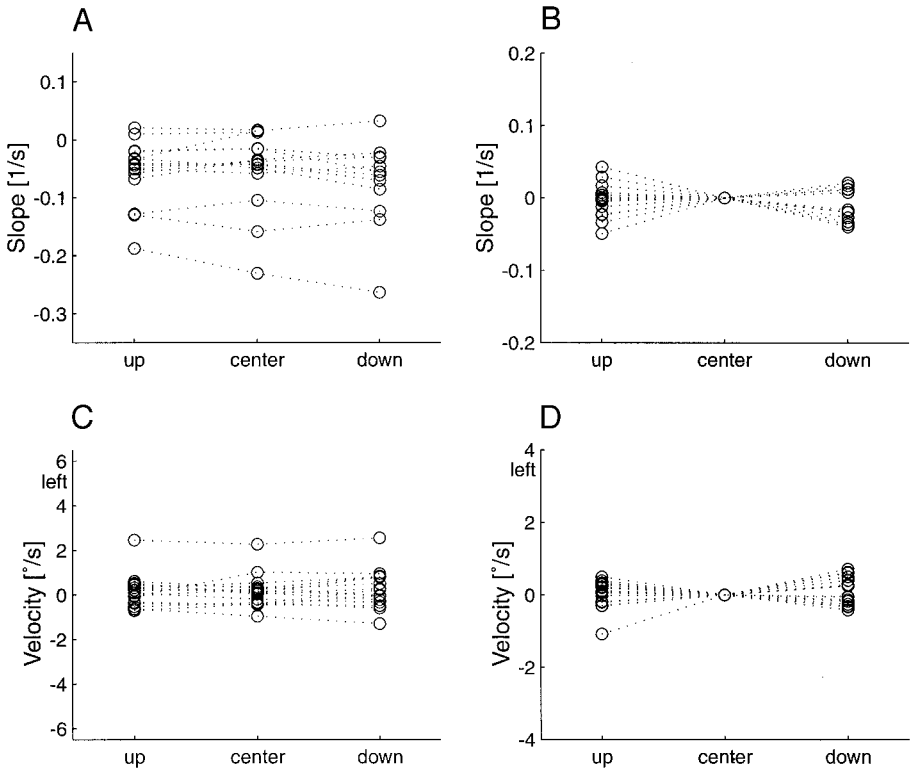

FIG. 5. Cerebellar patients, right eyes. Attempted fixations along horizontal lines. Abscissa: 20, 0, −20° vertical eccentricities. Data points of individual patients are connected by dashed lines. *A*: ω_z-r_z slopes of significant fits. *B*: differences of ω_z-r_z slopes from the values at 0° eccentricity. *C*: ω_z-r_z offsets. *D*: differences of ω_z-r_z offsets from the values at 0° eccentricity.

consistent velocity bias in the horizontal direction. In other words, there was no spontaneous horizontal nystagmus.

Torsional drift

In theory, it should be possible to determine if Alexander's law is valid in the torsional direction if torsional nystagmus is present. Because the range of torsional eye positions in which this nystagmus takes place is very limited, we were not able to fit significant first-order regressions between the torsional eye position and the torsional component of angular velocity. We also tried to determine if torsional drift velocity decreases exponentially with time during slow phases, which would be expected if the drift is caused by a leaky torsional velocity-to-position integrator. The limited torsional range, however, made such an analysis impossible.

Next we tried to determine if torsional drift depends on the horizontal and vertical eye position components. This was not a test for Alexander's law in the torsional direction, but a test to determine if the tendency of the eye to drift out of Listing's plane is a function of horizontal and vertical eye position.

Using the same data on which Fig. 3*A* is based (patient P8, right eye), Fig. 6 depicts the torsional angular drift velocity as a function of eye position along the vertical and horizontal meridians. While the negative ω_x-r_y slope was very small (Fig. 6*A*), there was a clear relation between ω_x and r_z (ω_x-r_z slope): in abduction (negative horizontal position), there was an intorsional drift and in adduction (positive horizontal position), an extorsional drift (Fig. 6*B*). The offsets in Fig. 6, *A* and *B*, are small, meaning that, in this patient, there was almost no torsional spontaneous nystagmus.

Figure 7, *A* and *B*, shows the ω_x-r_y slopes in the usual format for all patients. There was a considerable overlap between the

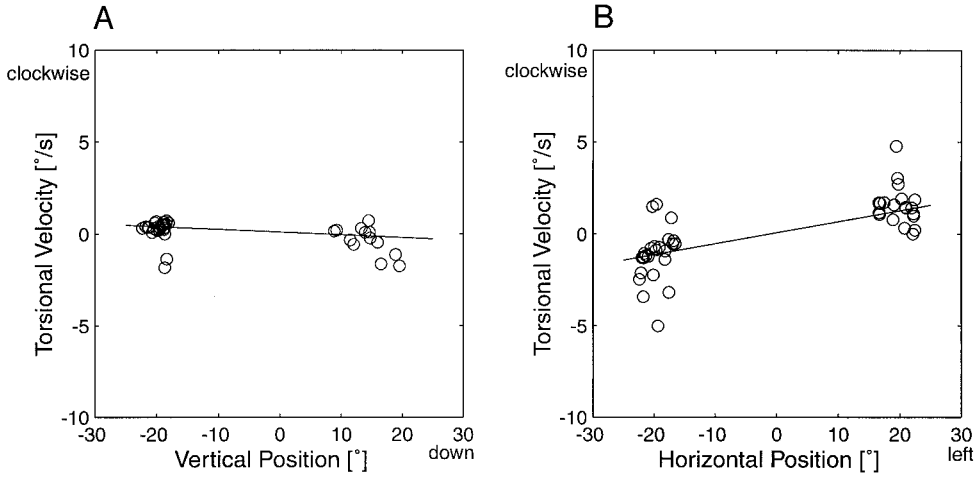

FIG. 6. Example of the relation between torsional components of angular velocity vectors (ordinate) and gaze eccentricity along the meridians (abscissa) (patient P8, right eye, same data as in Fig. 3*A*). *A*: torsional velocity vs. vertical eye position; slope = −0.015, offset = 0.1, $P < 0.001$. *B*: torsional velocity versus horizontal eye position; slope = 0.060, offset = 0.1, $P < 0.001$.

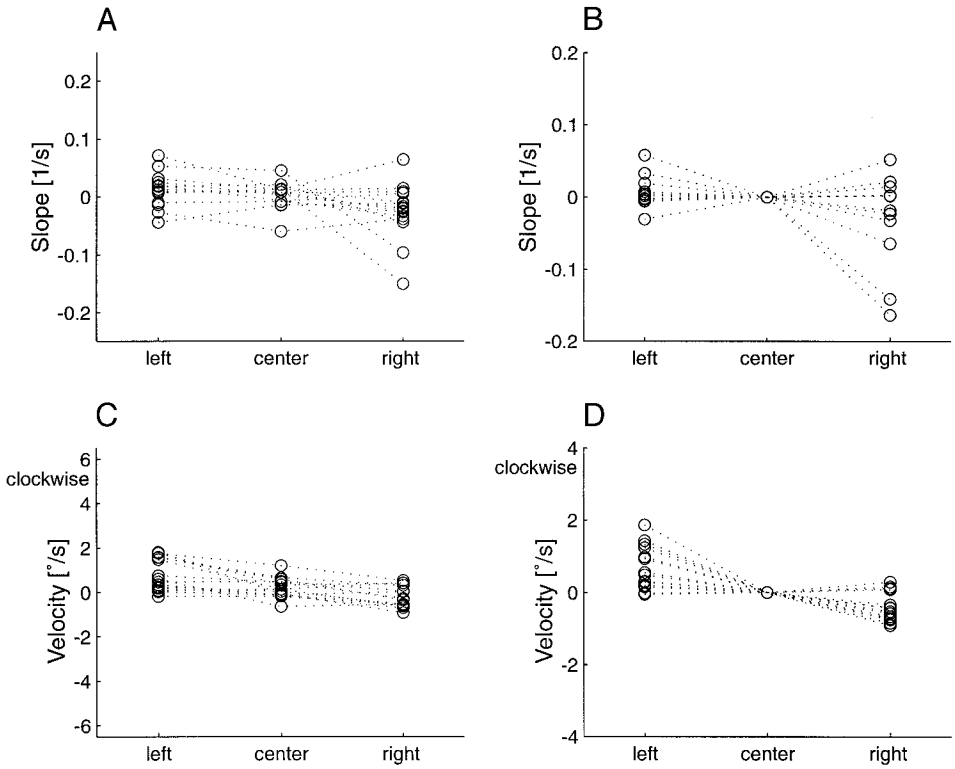

FIG. 7. Cerebellar patients, right eyes. Attempted fixations along vertical lines. Abscissa: 20, 0, −20° horizontal eccentricities. Data points of individual patients are connected by dashed lines. *A*: ω_x-r_y slopes of significant fits. *B*: differences of ω_x-r_y slopes from the values at 0° eccentricity. *C*: ω_x-r_y offsets. *D*: differences of ω_x-r_y offsets from the values at 0° eccentricity.

data points at the three horizontal directions (Fig. 7*A*). This is better visualized by subtracting the values obtained during fixations along the vertical meridian (Fig. 7*B*). For the pooled data, the ω_x-r_y slopes at the two horizontal gaze eccentricities were not significantly different from the slope at 0° [*t*-tests: *P* (right-center) = 0.552; *P* (left-center) = 0.075], but the differences between ω_x-r_y slopes at the two eccentric positions were significant [*t*-test: *P* (right-left) = 0.001], with the slopes being more positive in adduction.

Figure 7, *C* and *D*, shows the ω_x-r_y offsets at the different horizontal gaze eccentricities. There was a clear gradient of increasing extorsional velocity as the eyes moved left, i.e., toward adduction; on average, there was already an extorsional velocity bias at zero horizontal eccentricity, which corresponds to an extorsional spontaneous nystagmus (Fig. 7*C*). The gradient of ω_x-r_y offsets becomes even clearer when plotting the differences to the offsets at central fixation (Fig. 7*D*). For the pooled data, the differences between the three data sets were highly significant [*t*-tests: *P* (right-center) $<$ 0.001; *P* (left-center) $<$ 0.001; *P* (right-left) $<$ 0.001].

In Fig. 8, *A* and *B*, ω_x-r_z slopes are plotted with the line of sight pointing up, straight ahead, and down. As expected from Fig. 7, *C* and *D*, which shows a gradient of the ω_x-r_y offsets toward a drift in the extorsional direction when the eyes moved to the left (adduction), almost all eyes had positive ω_x-r_z slopes (Fig. 8*A*). There was no gradient of ω_x-r_z slopes as a function of vertical eccentricity (Fig. 8*B*). Accordingly, the differences between the three data sets were not significant for the pooled data [*t*-tests: *P* (up-center) = 0.106; *P* (up-down) = 0.597; *P* (center-down) = 0.858].

The ω_x-r_z offsets at different elevations are shown in Fig. 8, *C* and *D*. Data points were scattered around zero with averages slightly above zero for all three different vertical directions of the line of sight (Fig. 8*C*). There was no gradient of ω_x-r_z offsets as a function of vertical gaze eccentricity (Fig. 8*D*). Statistically, this was confirmed in that there were no significant differences between the three data sets [*t*-tests: *P* (up-center) = 0.388; *P* (up-down) = 0.591; *P* (center-down) = 0.921].

In summary, we found a significant gradient of torsional drift velocity in the horizontal direction: as the eyes adducted, extorsional drift increased. In many patients, a small extorsional drift was already present when the eyes looked straight ahead. There were no torsional drift gradients as a function of vertical position.

Is torsional drift independent from vertical drift?

In theory, torsional angular drift may simply be a result of cross-coupling from vertical angular drift. For instance, if the ocular rotation axis of a vertical drift changes with eye position, we expect an increasing torsional component of drift as a function of horizontal gaze eccentricity. Therefore, in each patient, we looked for correlations between torsional and vertical angular drift velocities. Note again that rotation and angular velocity vectors are, by definition, given in a head-fixed coordinate system (see METHODS), i.e., if a vector has a torsional component, the vector tilts out of the frontal head-fixed plane spanned by the vertical and horizontal axes.

We investigated possible cross-coupling effects between vertical and torsional drifts. Because the torsional drift in the straight-ahead gaze position is low, but increases as a function of horizontal gaze eccentricity, we studied the correlation between torsional and vertical drifts in 20° abduction and 20° adduction during attempted fixations along a vertical line. Figure 9*A* shows data from the same example given in Figs. 1, 2, and 3*A* (patient P8, right eye): torsional drift velocity is plotted against vertical drift velocity during 20° abduction and

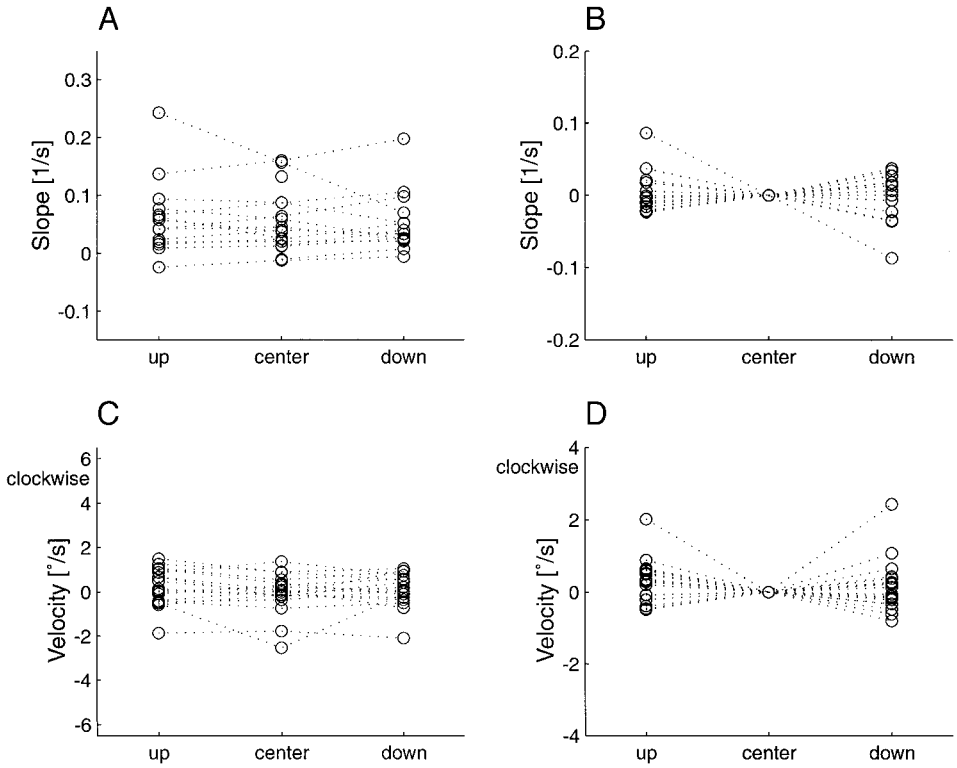

FIG. 8. Cerebellar patients, right eyes. Attempted fixations along horizontal lines. Abscissa: 20, 0, −20° vertical eccentricities. Data points of individual patients are connected by dashed lines. *A*: ω_x-r_z slopes of significant fits. *B*: differences of ω_x-r_z slopes from the values at 0° eccentricity. *C*: ω_x-r_z offsets. *D*: differences of ω_x-r_z offsets from the values at 0° eccentricity.

attempted vertical fixations (20° up, 20° down). There was a good correlation between torsional and vertical velocity in that the intorsional velocity decreased as upward velocity decreased. In this patient, however, the correlation between torsional and vertical velocity in adduction was not significant, but there was a tendency of extorsional velocity to decrease as upward velocity decreased (Fig. 9*C*). In the whole study population, 26 of 35 eyes showed a significant positive ω_x-ω_y slope during abduction, and 21 of 35 during adduction.

To test if this correlation between torsional and vertical angular velocity during fixations along vertical lines with eccentric horizontal gaze (abduction or adduction) was indeed caused by a cross-coupling of the two velocity components, or if it was only a result of individually different slopes between vertical eye position and torsional or vertical drift velocity, we plotted the ω_x-r_y and ω_y-r_y slopes of all patients against each other (Fig. 9, *B* and *D*). Both in abduction (Fig. 9*B*) and adduction (Fig. 9*D*), the slopes did not correlate significantly; ω_x-r_y slopes were scattered around zero whereas ω_y-r_y slopes were negative (Alexander's law) or positive (inverse Alexander's law). Therefore, torsional drift is not simply caused by a fixed cross-coupling of vertical drift, and the correlation between ω_x and ω_y in individual patients only reflects the fact that torsional velocity is modulated slightly by vertical eye position. If the velocity of torsional drift would mathematically depend on the velocity of vertical drift, e.g., via the half-angle rule, we would expect a similar correlation between ω_x and ω_y at a specific horizontal gaze eccentricity in all patients.

Another argument against torsional drift velocity being a result of a fixed cross-coupling with vertical drift velocity is shown in Fig. 10. Here we plotted the vertical-torsional drift direction of a patient's right eye (patient P8) as a function of horizontal eye position in upward (Fig. 10*A*) and in downward (Fig. 10*B*) gaze. The 0° vertical-torsional drift direction corresponds to a purely vertical drift whereas the +90° vertical-torsional drift is purely extorsional. In the following analyses, we call the slope of the linear regression between horizontal direction of gaze and vertical-torsional drift direction the *tilt angle coefficient* because it describes by how much the ocular rotation axis tilts in the horizontal plane as a function of the horizontal direction of the line of sight. If the tilt angle coefficient is zero, the ocular rotation axis stays head-fixed independent of the horizontal direction of gaze. A coefficient of 1 corresponds to an eye-fixed axis and a coefficient of 0.5 is necessary to follow Listing's law and, therefore, the half-angle rule. Clearly, in upward gaze, the tilt angle coefficient was much higher, and therefore close to eye-fixed (0.89), than in downward gaze, where it was close to head-fixed (0.19). This means that the torsional drift component relative to the vertical drift component was stronger in upward gaze than in downward gaze. Because for this patient Alexander's law was valid along the vertical direction, vertical velocity changed as a function of vertical eye position. On average, torsional drift velocity also changed somewhat, but less. Therefore the drift direction tilted toward more torsion as the eye was elevated.

Figure 10, *C* and *D*, summarizes the tilt angle coefficients of 10 of the 18 right eyes in which the slopes between horizontal eye position and vertical-torsional drift direction were significant in both upward and downward gaze. Five right eyes demonstrated Alexander's law (Fig. 10*C*), the remaining five demonstrated inverse Alexander's law (Fig. 10*D*) in the vertical direction. Clearly, the ocular rotation axis became more head-fixed as vertical gaze was moved in the direction in which vertical velocity increased. Some patients did not show this pattern, but in these cases the regressions were not significant, mainly because drift velocities were low and, therefore, vertical-torsional drift directions were noisy.

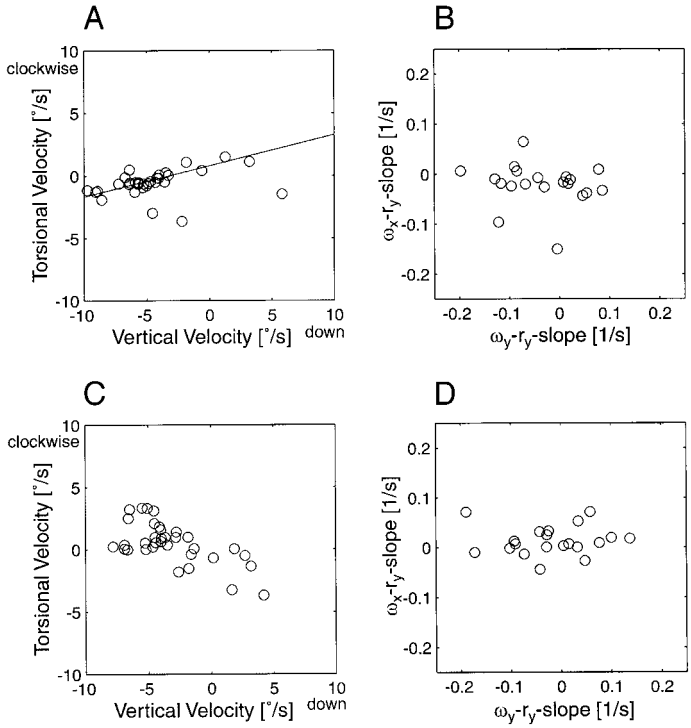

FIG. 9. Vertical and torsional components of nystagmus slow phases. *A*: patient P8, right eye (same trial as in Figs. 1, 2, and 3*A*). Torsional vs. vertical angular velocity components of nystagmus slow phases during 20° abduction and attempted vertical fixations (20° upward, 20° downward); slope = 0.246, offset = 0.7861, $P < 0.001$. *B*: ω_x-r_y slopes vs. ω_y-r_y slopes in all patients (right eyes) during 20° abduction and attempted vertical fixations; regression not significant ($P = 0.532$). *C*: patient P8, right eye (same trial as in Figs. 1, 2, and 3*A*). Torsional vs. vertical angular velocity components of nystagmus slow phases during 20° adduction and attempted vertical fixations; regression not significant ($P = 0.094$). *D*: ω_x-r_y slopes vs. ω_y-r_y slopes in all patients (right eyes) during 20° adduction and attempted vertical fixations; regression not significant ($P = 0.890$).

Is torsional drift independent from horizontal drift?

This subsection follows the same logic as *Is torsional drift independent from vertical drift?* We attempted to determine if torsional angular drift is a result of a fixed cross-coupling with horizontal angular drift. Because both torsional and horizontal angular drift increased with horizontal gaze eccentricity, the correlation between the two velocity components was, as expected, typically significant in 15 of the 18 right eyes and 14 of the 17 left eyes. Figure 11*A* depicts the correlation between these two parameters for patient P8 (right eye).

To investigate whether or not these significant individual correlations between torsional and horizontal angular velocity during fixations along the horizontal meridian are caused by a fixed cross-coupling of the two velocity components, or are only a result of individually different slopes between horizontal eye position and torsional or horizontal drift velocity, we plotted the ω_x-r_z and ω_z-r_z slopes of all right eyes against each other (Fig. 11*B*). Because the adducting horizontal drift (positive sign) increased as the eye abducted (negative sign), and the extorsional drift increased (positive sign) as the eye adducted (positive sign), data points are scattered in the upper left quadrant. However, there was no significant correlation between the slopes, which indicates that the torsional drift was independent from the horizontal drift, even though they correlated in individual patients, because of the horizontal-eye-position dependence of both drifts. Therefore, the torsional drift is not caused by a fixed cross-coupling from the horizontal drift, and the correlation between ω_x and ω_z in individual patients only reflects the fact that both torsional and horizontal velocity were modulated by horizontal eye position.

We also investigated whether or not there were consistent gradients between the horizontal-torsional drift direction and the gaze elevation in abduction and adduction. Significant gradients could be seen in most eyes (33 of 35 eyes in abduction, 34 of 35 in adduction), but the magnitudes and signs of these gradients showed no pattern. In only a minority of eyes (12 of 35), the gradients between horizontal-torsional drift direction and vertical gaze direction had the same sign in abduction and adduction.

Does vertical drift obey Listing's law?

To interpret further the patterns of vertical drift in our patients, we developed a theoretical scheme of the predicted effects of different types of abnormalities on the directions and eye-position dependence of vertical-torsional drift. Figure 12 depicts four possible relations between torsional and vertical drift angular velocities. Figure 12, *A*, *C*, *E*, and *G*, shows vertical angular drift velocity as a function of torsional angular drift velocity; Fig. 12, *B*, *D*, *F*, and *H*, shows vertical-torsional

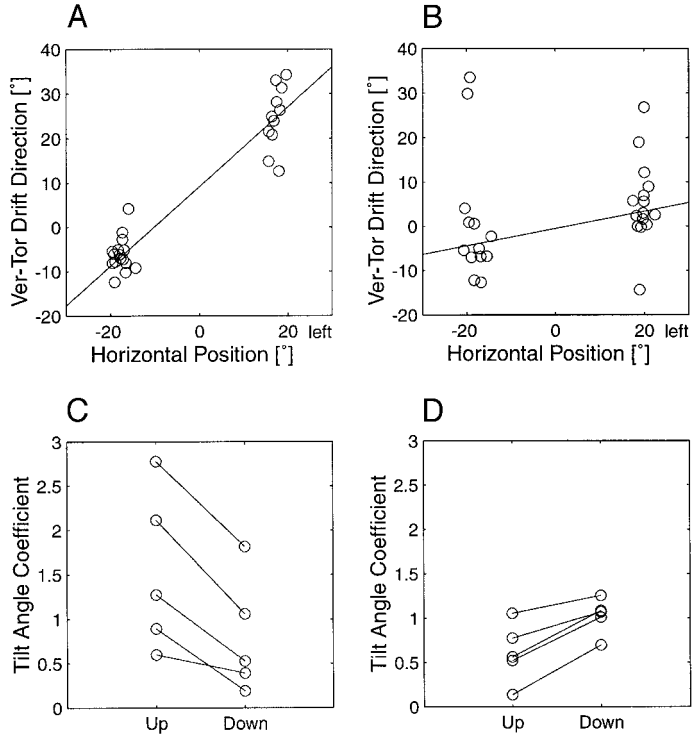

FIG. 10. Vertical-torsional drift directions and tilt angle coefficients. *A*: patient P8, right eye (same trial as in Figs. 1; 2; 3*A*; and 9, *A* and *C*). Vertical-torsional drift direction as a function of horizontal position in 20° upward gaze. The regression line (solid) was determined by an iterative linear fit whereby the most distant point from the line was discarded each time; the iteration was stopped after 20% of the data points were rejected. Slope ("tilt angle coefficient") = 0.89, offset = 9.2. *B*: same as in *A* but in 20° downward gaze. Slope (tilt angle coefficient) = 0.19, offset = −0.5. *C*: tilt angle coefficients in 5 patients (right eyes) that showed Alexander's law of vertical drift. Solid lines connect data points of individuals in upward (Up) and downward (Down) gaze. *D*: same as in *C* but with data from 5 other patients (right eyes) with inverse Alexander's law of vertical drift.

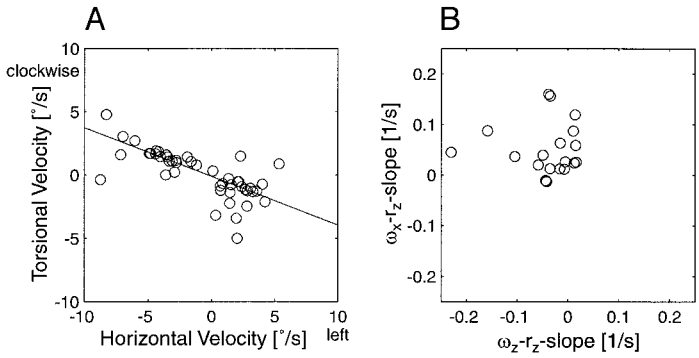

FIG. 11. Horizontal and torsional components of nystagmus slow phases. *A*: patient P8, right eye (same trial as in Figs. 1; 2; 3*A*; 9, *A* and *C*; and 10, *A* and *B*). Torsional vs. horizontal angular velocity components of nystagmus slow phases during attempted eccentric fixations along the horizontal meridian (20° rightward, 20° leftward). Slope = −0.385, offset = −0.111, $P < 0.001$. *B*: ω_x-r_z slopes vs. ω_z-r_z slopes in all patients (right eyes) during attempted eccentric fixations along the horizontal meridian; regression not significant ($P = 0.214$).

drift direction (in polar coordinates) as a function of horizontal eye position. In each panel, four data points are depicted: when the patient is looking 20° right and 20° up (▲), when the patient is looking 20° right and 20° down (▼), when the patient is looking 20° left and 20° up (△), and when the patient is looking 20° left and 20° down (▽). In some instances (Fig. 12, *B–D*), data points during upward and downward viewing overlap (producing hexagrams). In the *left* panels, we connected the points with the same horizontal eccentricity; in the *right* panels, the points with the same vertical eccentricity.

Figure 12*A* shows vertical drift caused by a leaky vertical velocity-to-position integration; this drift, we assume, obeys Listing's law, i.e., the half-angle rule. Consequently, there is a torsional drift component that depends on the vertical drift velocity (3°/s at 20° vertical gaze eccentricity) and the horizontal gaze eccentricity (20°). The lines connecting the drift directions during rightward and leftward viewing superimpose in upward and downward gaze; the slope of both lines is 0.5 according to the half-angle rule (Fig. 12*B*).

Figure 12*C* depicts a situation with an upward vertical drift (−5°/s) of purely vestibular origin that, we assume, shows no eye position dependence (i.e., is head-fixed). Therefore, in no direction of gaze is there a torsional drift component (Fig. 12*D*). The slope between drift directions during rightward and leftward viewing is 0 and the lines superimpose in upward and downward gaze.

Figure 12*E* combines the situations from Fig. 12, *A* and *C*, i.e., we added together the vertical leaky integrator drift, which obeys Listing's law, and the upward bias drift, which is independent of vertical eye position and does not include a torsional component in any direction of gaze. As a consequence, the slopes between the vertical-torsional drift directions during abduction and adduction are different between upward and downward gaze (Fig. 12*F*).

In Fig. 12*G* we added the type of torsional drift that we found in the patients. This torsional drift depends on horizontal eye position and is intorsional in abduction (in this example, −1°/s during 20° abduction) and extorsional in adduction (in this example, 1°/s during 20° adduction). This leads to an additional change of the slopes of the lines between vertical-torsional drift direction during abduction and adduction in both upward and downward gaze.

This theoretical example demonstrates that we cannot simply examine the vertical-torsional drift directions to decide whether or not leaky velocity-to-position integration in the vertical direction leads to drift movements following Listing's law. To test this question correctly, the *slopes* between vertical position and torsional or vertical angular drift (ω_x-r_y slope and ω_y-r_y slope) must be analyzed, both of which reflect the drift induced by leaky integration when the eye is moved in a vertical direction. Assuming that Listing's law is adhered to by the drift caused by leaky vertical velocity-to-position integration alone (i.e., there is no vertical velocity bias), the coefficient c_{xy} = (ω_x-r_y slope/ω_y-r_y slope) will increase as a function of horizontal eccentricity (abduction and adduction). It can easily be shown that c_{xy} coincides with the horizontal component r_z of the current ocular rotation vector, provided Listing's law is valid:

$$c_{xy} = r_z$$

e.g., at 20° horizontal gaze eccentricity, $c_{xy} = 0.175$. This value corresponds to a tilt of the angular rotation axis in the direction of gaze by 10°, according to the half-angle rule.

Figure 13 shows, for all right eyes, ω_y-r_y slopes compared

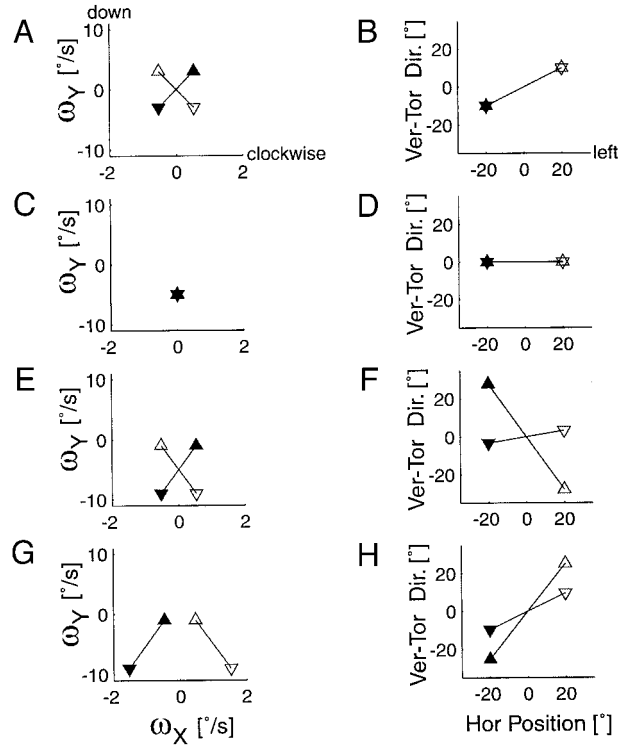

FIG. 12. Theoretical scheme of possible relations between torsional and vertical drift angular velocities. ▲, eye position 20° right/20° up. ▼, eye position 20° right/20° down. △, 20° left/20° up. ▽, 20° left/20° down. Overlying upward and downward data points produce hexagrams. *A, C, E, G*: vertical angular drift velocity as a function of torsional angular drift velocity. Data points with the same horizontal eccentricity are connected. *B, D, F, H*: vertical-torsional drift direction in polar coordinates as a function of horizontal eye position. Data points with the same vertical eccentricity are connected. *A, B*: vertical drift in Listing's plane caused by leaky vertical velocity-to-position integration. *C, D*: vertical drift with no eye position dependence. *E, F*: summation of the vertical drifts in (*A, B*) and (*C, D*). *G, H*: summation of the vertical drift in (*E, F*) and horizontal-eye-position–dependent torsional drift.

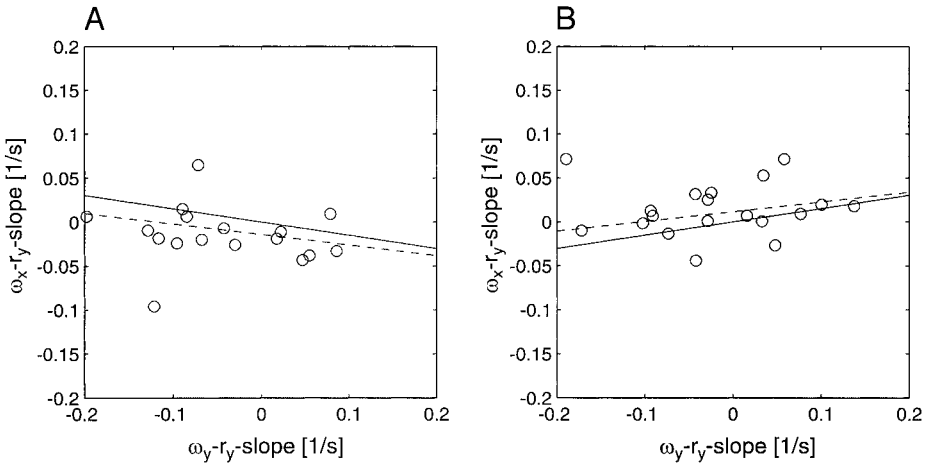

FIG. 13. Cerebellar patients, right eyes, ω_y-r_y slopes vs. ω_x-r_y slopes. Data points are plotted for which the ω_y-r_y slopes were significant ($P < 0.05$). The solid lines (slope = ± 0.15) indicate where the data points must lie at a horizontal gaze eccentricity of 17.3° to obey Listing's law. The dashed lines indicate a robust linear regression of the data whereby 20% of the points were discarded (same procedure as in Fig. 10). *A*: data points in abduction. Slope of solid line $c_{xy} = -0.15$; confidence interval ($P < 0.05$) of robust linear fit = (−0.289, 0.049); $R^2 = 0.378$. *B*: data points in adduction. Slope of solid line $c_{xy} = 0.15$; confidence interval ($P < 0.05$) of robust linear fit = (−0.059, 0.280); $R^2 = 0.327$.

with ω_x-r_y slopes in abduction (*A*) and adduction (*B*). Only data points for which the ω_y-r_y slopes were significant are plotted. The solid lines ($c_{xy} = \pm 0.15$) indicate where the data points are expected to lie at a horizontal gaze eccentricity of 17.3°, which was the average eye position that patients achieved during attempted horizontal fixation. (Note that in most patients there was an ongoing horizontal gaze-evoked nystagmus that led to horizontal eye positions below the attempted 20°.)

In abduction (Fig. 13*A*), ω_x-r_y slopes decrease with increasing ω_y-r_y slopes whereas in adduction (Fig. 13*B*), ω_x-r_y slopes increase with increasing ω_y-r_y slopes. The null hypothesis that the regressions through the data points were not different from the expected regressions with slopes of −0.15 or 0.15, respectively, could not be rejected ($P > 0.05$). The same was the case for the population of left eyes. Thus it can be inferred that leaky vertical integration alone leads to drift movements that do not violate Listing's law.

Does horizontal drift obey Listing's law?

We have already demonstrated that for our cerebellar patients there was no consistent velocity bias component to the ocular drift in the horizontal direction (Fig. 5). Therefore it can be inferred that horizontal drift in the cerebellar patients was mainly caused by leaky horizontal velocity-to-position integration. To investigate whether or not these horizontal drift movements were in accordance with Listing's law, we plotted the *slopes* between horizontal position and torsional or horizontal angular drift (ω_x-r_z slope and ω_z-r_z slope), both of which reflect the drift induced by leaky integration when the eye is moved in a horizontal direction. Assuming that Listing's law is adhered to by the drift caused by leaky horizontal velocity-to-position integration alone (i.e., there is no horizontal velocity bias), the coefficient c_{xz} = (ω_x-r_z slope/ω_z-r_z slope) will change as a function of vertical eccentricity (upward gaze and downward gaze). Coefficient c_{xz} coincides with the vertical component r_y of the current ocular rotation vector, provided Listing's law is valid:

$$c_{xz} = r_y$$

Figure 14 plots, for all right eyes, ω_y-r_z slopes against ω_x-r_z slopes in upward gaze (*A*) and downward gaze (*B*). Only data points for which the ω_z-r_z slopes were significant are plotted. The solid lines (in upward gaze $c_{xz} = -0.19$; in downward gaze $c_{xz} = 0.15$) indicate where the data points are expected to lie at an upward eccentricity of 21.2° and a downward eccentricity of 16.8°, respectively, which were the average eye positions that patients achieved during attempted vertical fixation. (Note that in most patients there was an ongoing upward drift that led to these average eye positions that differed from the attempted 20°.)

Clearly, in both upward gaze (Fig. 14*A*) and downward gaze (Fig. 14*B*), the relation between ω_z-r_z and ω_x-r_z slopes did not

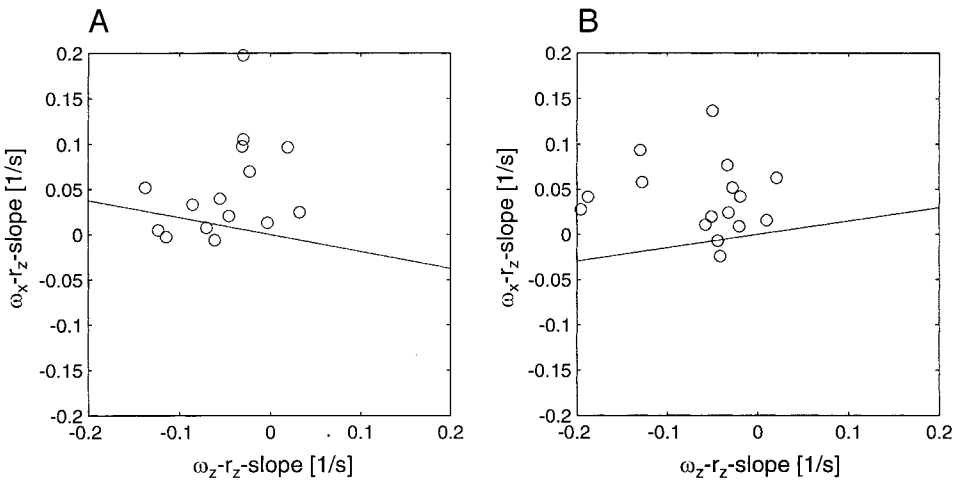

FIG. 14. Cerebellar patients, right eyes, ω_z-r_z slopes vs. ω_x-r_z slopes. Data points are plotted for which the ω_z-r_z slopes were significant ($P < 0.05$). The solid lines indicate where the data points must lie at an upward gaze eccentricity of 21.2° (*A*) and a downward gaze eccentricity of 16.8° (*B*) to obey Listing's law. Regressions are not shown ($R^2 < 0.1$). *A*: data points in upward gaze. Slope of solid line $c_{xz} = -0.19$. *B*: data points in downward gaze. Slope of solid line $c_{xz} = 0.15$.

fit the prediction. The same was the case for the population of left eyes. This result could be expected because, as already demonstrated in Fig. 8, both torsional and horizontal drift velocity increased with horizontal eye eccentricity. However, this does not mean that a leaky horizontal velocity-to-position integrator leads to drift movements that per se violate Listing's law. Such a conclusion could only been drawn if, in the majority of patients, there was a fixed mathematical relation between torsional angular drift and horizontal angular drift, which was not the case (see Figs. 11 and 14).

Finally, we investigated whether or not the kinematics of the horizontal drift would produce an additional torsional component when patients looked upward or downward. In this case, in accordance with the half-angle rule, ω_x-r_z slopes in upward gaze should be smaller than in downward gaze. As already demonstrated in Fig. 8*B*, no significant vertical gradient of ω_x-r_z slopes could be found.

DISCUSSION

Summary of experimental findings

In a population of 18 patients with horizontal gaze-evoked and downbeat nystagmus caused by cerebellar atrophy, we analyzed the three-dimensional kinematics of eye drift. The overall ocular drift in these patients was composed of three independent components: *1*) an upward drift, *2*) a horizontal centripetal drift, and *3*) a torsional drift that increased with horizontal eye eccentricity.

The *vertical drift* itself could be divided into two subcomponents: a drift that increased with vertical eccentricity, according to Alexander's law (Alexander 1912; Robinson et al. 1984), and a drift that was independent of vertical eye position. Because of this upward-directed velocity bias, the vertical eye position at which there was no vertical drift (null position) was moved upward, in most cases even beyond the normal vertical range of eye movements. The increase of upward drift velocity with eccentric horizontal gaze, a prominent feature of downbeat nystagmus, was caused by an increase of the velocity bias and not an increased slope of the vertical eccentricity-dependent drift.

The *horizontal drift* increased with horizontal gaze eccentricity, according to Alexander's law. There was no significant velocity bias of horizontal drift, i.e., no consistent horizontal spontaneous nystagmus was present.

The *torsional drift* also increased with horizontal gaze eccentricity and we therefore called it *horizontal-eye-position–dependent torsional drift*. In abduction, this drift was intorsional and in adduction, extorsional. There was a small extorsional velocity bias, i.e., when patients looked straight ahead, both eyes drifted somewhat in the extorsional direction. (The analysis of disconjugate eye movements in cerebellar patients is not the topic of this study.) Because of the small torsional range of eye movements during downbeat nystagmus, we were not able to decide whether or not the torsional drift velocity depended on the torsional eye position.

Mechanism of vertical drift

Any plausible hypothesis of why there usually is downbeat nystagmus in the presence of cerebellar atrophy must explain both the upward-directed velocity bias *and* the vertical drift that increases with vertical gaze eccentricity. The upward-directed velocity bias could be caused by central ocular motor pathways that are asymmetrically implemented for the vertical movement plane; the intact cerebellum would usually inhibit the dominating upward pathways but, in the case of cerebellar failure, this asymmetry would be unmasked (Ito et al. 1977). Alternatively, cerebellar atrophy could affect central ocular pathways for movements mainly in the downward direction but less in the upward direction (Baloh and Spooner 1981). In both hypotheses, it remains unclear if the superimposed vertical gaze-dependent centripetal ocular drift is directly related to the vertical velocity bias or is a result of a coexisting disorder of the vertical velocity-to-position integrator, which is also affected by cerebellar atrophy.

A hypothesis concerning the mechanism of downbeat nystagmus that has been proposed by Böhmer and Straumann (1998) is based on the fact that the semicircular canals are asymmetric in the vertical direction: if the sensitivity vectors of all six semicircular canals, as anatomically measured by Blanks et al. (1975), are arithmetically added, the resultant vector could lead to upward-directed ocular drift. This vertical asymmetry is mainly caused by the fact that the anterior canals form a smaller angle with the sagittal plane of the head than do the posterior canals. An intact cerebellum would, by way of the flocculus/paraflocculus, suppress this upward drift but, as cerebellar function fails, the upward eye-position–independent ocular drift would become manifest. If this vertical velocity bias in the upward direction is added to the effect of the reduced time constant of the velocity-to-position integrator, which also might be caused by the floccular/parafloccular impairment, Alexander's law is found to be valid in the vertical direction. The fact that some patients show an inverse Alexanders's law could simply be the result of an unstable rather than a leaky integrator (Zee et al. 1981).

The observation that in most patients the upward velocity bias increased with lateral gaze is not explained by the hypothesis of Böhmer and Straumann (1998). This phenomenon could, for instance, be the result of an erroneous distance correction by the vestibular system such that, during eccentric gaze, the desired point of regard is perceived to be closer on eccentric than on straight-ahead gaze, leading to a spurious increase in the gain of the vestibular signal responsible for the vertical velocity bias.

Mechanism of horizontal drift

The existence of horizontal gaze-evoked nystagmus is simply a result of the decreased time constant of the velocity-to-position integrator in the horizontal direction. As a result, Alexander's law is usually valid for this type of horizontal drift. It is known from experimental and clinical studies that horizontal gaze-evoked nystagmus in cerebellar disease is a result of reduced floccular/parafloccular function (Zee et al. 1981).

Mechanism of torsional drift

Horizontal-eye-position–dependent torsional drift can be viewed as the consequence of deficient mapping of a torsional eye position signal to the current direction of gaze. The magnitude of the torsional signal that would be needed to imple-

ment Listing's law would vary as a function of the direction of the line of sight (horizontal and vertical eye position). Normally, this mapped torsional signal would encode the difference between the mechanically determined torsional resting position of the eye and the torsional ocular position required by Listing's law. Because this difference probably changes with changing eye position, it can be expected that, if the brain did not generate the correct torsional tonic signal, the velocity of the torsional drift would vary as a function of the line of sight. Therefore, the eyes would always drift from the Listing's plane defined by the saccadic system (pulse) to torsional positions defined by the ocular plant. The torsional components of quick phases would then move the eyes back to or even beyond Listing's plane to correct the drifts out of Listing's plane (Lee et al. 1998; Van Opstal et al. 1996). This scheme does not exclude the idea that the ocular plant restricts three-dimensional eye positions in a planar fashion, but such a mechanically implemented plane would at least have a different orientation than the neurally-defined Listing's plane. More specifically, the "mechanical plane" would be tilted less backward than Listing's plane because during adduction the eyes drift in the extorsional direction, and during abduction they drift in the intorsional direction. Of course, the ocular plant might also implement a nonplanar surface toward which the eyes would drift when the mapping of the tonic torsional signal to the direction of gaze is deficient. The fact that, with gaze straight ahead, there was a small extorsional drift (spontaneous intorsional nystagmus) might be related to the finding by Seidman et al. (1995) that the time constant of torsional drift after a mechanically applied extorsion is less than half that from intorsion.

Another possibility is that torsional drift is a result of abnormally large torsional blips that occur during the quick phases. After these blips, which violate Listing's law, the eyes would drift back to Listing's plane. We cannot completely exclude such a mechanism, but in this case the expectation would be that the standard deviation of data points from the plane fitted to the presaccadic eye positions should be smaller than the standard deviation from the plane fitted to the postsaccadic eye positions; this, however, was not the case (Table 1).

Validity of Listing's law

In the absence of vestibular stimulation, the intact ocular motor system closely obeys Listing's law during fixations and, to a lesser degree, during smooth pursuit eye movements and saccades (Haslwanter et al. 1991; Straumann et al. 1996; Tweed and Vilis 1990; Tweed et al. 1992). Torsional velocity-to-position integration, together with vertical integration, is located predominantly in the interstitial nucleus of Cajal (iC), which is the source of the appropriate vertical and torsional eye position signals that are transmitted to the ocular motor neurons. Unilateral lesions or microstimulations of the iC lead to movements out of Listing's plane (Crawford et al. 1991). Similarly, unilateral lesions and microstimulations of the rostral interstitial nucleus of the medial longitudinal fascicle (riMLF), which contains the premotor vertical-torsional saccadic short-lead burst neurons, lead to eye movements out of Listing's plane (Crawford and Vilis 1992; Henn et al. 1991; Suzuki et al. 1995). After a saccade, a small torsional position error can occur, but it is corrected during the subsequent saccade. It has been shown in rhesus monkeys that the nucleus reticularis tegmenti pontis (NRTP), which provides input to the cerebellum, plays an important role in this strategy of stabilizing Listing's plane (Van Opstal et al. 1996). Thus it is conceivable that the cerebellum influences the above brain stem structures involved in controlling the torsional degree of freedom of the eye and, therefore, Listing's law. In the case of cerebellar atrophy, we therefore can expect violations of Listing's law.

Indeed, the ocular drift in our cerebellar patients violated Listing's law. This was partly caused by a torsional drift that depended on horizontal gaze eccentricity and changed its direction if the eyes abducted or adducted. We propose that, in normal subjects, the cerebellum generates a tonic torsional signal that maintains the eyes in Listing's plane against the mechanical forces of the ocular plant. Because, in our hypothesis, the difference between the mechanically determined torsional zero position and the torsional zero position defined by Listing's law varies with the direction of the line of sight, the tonic torsional signal must be mapped as a function of horizontal-vertical eye position. Because of this eye-position dependence, the tonic torsional signal cannot simply be the output of a torsional velocity-to-position integrator. Therefore, the normal cerebellum does more than just maintain the time constants of the integrators or compensate for imbalances of signals from the semicircular canals. By taking into account the instantaneous horizontal and vertical eye position components, it produces the correct torsional position component, i.e., actively controls the three-dimensional kinematics of the eye. If this torsional mapping does not occur, eye-position–dependent torsional drift is expected. We consider this drift a "passive" violation of Listing's law because we assume that the drift is determined by the mechanics of the ocular motor plant in the absence of a mapped torsional tonic signal. All other known violations of Listing's law are caused by mechanisms that structurally (e.g., orbital tumors) or by explicit neural signals (e.g., torsional macroblips, eye movements evoked by torsional vestibular stimulation) interfere with Listing's law.

We also investigated whether or not vertical drift in isolation would conform with Listing's law. The data showed that this was not case. However, if we only analyzed the vertical drift component caused by leaky vertical integration, eye trajectories did not significantly violate the half-angle rule and, therefore, obeyed Listing's law. So it appears that the vertical velocity-to-position integrator encodes vertical eye position in Listing's plane, but that the vertical velocity bias drives the eye out of Listing's plane, in addition to the torsional drift that depends on horizontal eye position. The fact that the vertical velocity bias violates Listing's law supports the hypothesis that this signal is of vestibular origin, because a distinct property of eye movements evoked by vestibular stimulation is that the axis tilts less in the direction of gaze than required by the half-angle rule (Misslisch et al. 1994, Palla et al. 1999). That the vertical velocity bias comes from the pursuit system is unlikely because smooth pursuit eye movements obey Listing's law (Haslwanter et al. 1991; Tweed et al. 1992). Whether or not the horizontal centripetal drift in isolation violated Listing's law could not be decided based on our measurements because torsional drift also increased as a function of horizontal eye position with a slope that was different in each patient.

Finally, we investigated whether or not horizontal-eye-position–dependent torsional drift could also occur in isolation without the presence of horizontal gaze-evoked nystagmus and downbeat nystagmus. Because our patients were selected on the basis that horizontal gaze-evoked and downbeat nystagmus were present, we cannot give a conclusive answer. It is our clinical experience, however, that patients with slight cerebellar atrophy often, in the absence of horizontal gaze-evoked nystagmus or downbeat nystagmus, show torsional instability with a tendency to drift during eccentric gaze: the eyes slowly move extorsionally during adduction and intorsionally during abduction. This pattern is consistent with the results on torsional drift for the patients presented. Our clinical experience also supports the hypothesis that torsional mapping of the eye to implement Listing's law is a separate mechanism than that for maintaining horizontal and vertical gaze.

In conclusion, the three-dimensional kinematic analysis of ocular drift in patients with cerebellar atrophy strongly suggests that the cerebellum is involved in the neural implementation of Listing's law.

The field coil systems (a modification of a Remmel-type system) used in this study were designed and constructed by A. G. Lasker. Paradigms were programmed by D. Roberts. Some of the patients were recruited by P. D. Kramer, R. F. Lewis, and S. G. Reich.

This work was supported by the Swiss National Science Foundation (3231-051938.97/3200-052187.97), National Eye Institute Grant EY-O1849, the Betty and David Koetser Foundation for Brain Research, and the Arnold-Chiari Foundation. Address for reprint requests: D. Straumann, Neurology Dept., Zurich University Hospital, CH-8091 Zurich, Switzerland.

Received 23 June 1999; accepted in final form 8 October 1999.

REFERENCES

ALEXANDER, G. Die Ohrenkrankheiten im Kindesalter. In: *Handbuch der Kinderheilkunde,* edited by M. Pfaundler and A. Schlossmann. Leipzig: Vogel, 1912, p. 84–96.

BALOH, R. W. AND SPOONER, J. W. Downbeat nystagmus: a type of central vestibular nystagmus. *Neurology* 31: 304–10, 1981.

BLANKS, R.H.I., CURTHOYS, I. S., AND MARKHAM, C. H. Planar relationships of the semicircular canals in man. *Acta Otolaryngol. (Stockh.)* 80: 185–196, 1975.

BÖHMER, A. AND STRAUMANN, D. Pathomechanism of mammalian downbeat nystagmus due to cerebellar lesion—a simple hypothesis. *Neurosci. Lett.* 250: 127–130, 1998.

CRAWFORD, J. D., CADERA, W., AND VILIS, T. Generation of torsional and vertical eye position signals by the interstitial nucleus of Cajal. *Science* 252: 1551–1553, 1991.

CRAWFORD, J. D. AND VILIS, T. Axes of eye rotation and Listing's law during rotations of the head. *J. Neurophysiol.* 65: 407–423, 1991.

CRAWFORD, J. D. AND VILIS, T. Symmetry of oculomotor burst neuron coordinates about Listing's plane. *J. Neurophysiol.* 68: 432–448, 1992.

DONDERS, F. C. Beiträge zur Lehre von den Bewegungen des menschlichen Auges. *Holländ Beitr. Anat. Physiol. Wiss.* 1: 105–145, 1848.

FETTER, M. AND SIEVERING, D. Three-dimensional eye movement analysis in benign paroxysmal positioning vertigo and nystagmus. *Acta Otolaryngol. (Stockh.)* 115: 353–357, 1995.

HASLWANTER, T., STRAUMANN, D., HEPP, K., HESS, B.J.M., AND HENN, V. Smooth pursuit eye movements obey Listing's law in the monkey. *Exp. Brain Res.* 87: 470–472, 1991.

HAUSTEIN, W. Considerations on Listing's law and the primary position by means of a matrix description of eye position control. *Biol. Cybern.* 60: 411–420, 1989.

HELMCHEN, C., GLASAUER, S., AND BÜTTNER, U. Pathological torsional eye deviation during voluntary saccades: a violation of Listing's law. *J. Neurol. Neurosurg. Psychiatry* 62: 253–260, 1997.

HELMHOLTZ, H. V. *Handbuch der Physiologischen Optik.* Hamburg: Voss, 1867.

HENN, V., STRAUMANN, D., HESS, B. J., HEPP, K., VILIS, T., AND REISINE, H. Generation of vertical and torsional rapid eye movement in the rostral mesencephalon. Experimental data and clinical implications. *Acta Otolaryngol. (Stockh.) Suppl.* 481: 191–193, 1991.

HEPP, K. On Listing's law. *Comm. Math. Phys.* 132: 285–292, 1990.

HESS, K., DURSTELER, M. R., AND REISINE, H. Analysis of slow phase eye velocity during the course of an acute vestibulopathy. *Acta Otolaryngol. (Stockh.)* 406: 227–230, 1984.

HORE, J., WATTS, S., AND VILIS, T. Constraints on arm position when pointing in three dimensions: Donders' law and the Fick gimbal strategy. *J. Neurophysiol.* 68: 374–383, 1992.

ITO, M., NISIMARU, N., AND YAMAMOTO, M. Specific patterns of neuronal connexions involved in the control of the rabbit's vestibulo-ocular reflexes by the cerebellar flocculus. *J. Physiol. (Lond.)* 265: 833–854, 1977.

LEE, C., STRAUMANN, D., AND ZEE, D. S. Saccades from torsional offset positions back to Listing's plane. *Soc. Neurosci. Abstr.* 24: 1744, 1998.

LEIGH, R. J. AND ZEE, D. S. *The Neurology of Eye Movements.* New York: Oxford, 1999.

MISSLISCH, H., TWEED, D., FETTER, M., SIEVERING, D., AND KOENIG, E. Rotational kinematics of the human vestibuloocular reflex. III. Listing's law. *J. Neurophysiol.* 72: 2490–2502, 1994.

PALLA, A., STRAUMANN, D., AND OBZINA, H. Eye position dependence of three-dimensional ocular rotation axis orientation during head impulses in humans. *Exp. Brain. Res.* 129: 127–133, 1999.

QUAIA, C. AND OPTICAN, L. M. Commutative saccadic generator is sufficient to control a 3-D ocular plant with pulleys. *J. Neurophysiol.* 79: 3197–3215, 1998.

ROBINSON, D. A., ZEE, D. S., HAIN, T. C., HOLMES, A., AND ROSENBERG, L. F. Alexander's law: its behavior and origin in the human vestibulo-ocular reflex. *Ann. Neurol.* 16: 714–722, 1984.

SCHNABOLK, C. AND RAPHAN, T. Modeling three-dimensional velocity-to-position transformation in oculomotor control. *J. Neurophysiol.* 71: 623–638, 1994.

SEIDMAN, S. H., LEIGH, R. J., TOMSAK, R. L., GRANT, M. P., AND DELL'OSSO, L. F. Dynamic properties of the human vestibulo-ocular reflex during head rotations in roll. *Vision Res.* 35: 679–689, 1995.

STRAUMANN, D. AND ZEE, D. S. Three-dimensional aspects of eye movements. *Curr. Opin. Neurol.* 8: 69–71, 1995.

STRAUMANN, D., ZEE, D. S., SOLOMON, D., AND KRAMER, P. D. Validity of Listing's law during fixations, saccades, smooth pursuit eye. *Exp. Brain Res.* 112: 135–146, 1996.

STRAUMANN, D., ZEE, D. S., SOLOMON, D., LASKER, A. G., AND ROBERTS, D. Transient torsion during and after saccades. *Vision Res.* 35: 3321–3334, 1995.

SUZUKI, Y., BÜTTNER-ENNEVER, J. A., STRAUMANN, D., HEPP, K., HESS, B. J., AND HENN, V. Deficits in torsional and vertical rapid eye movements and shift of Listing's plane after uni- and bilateral lesions of the rostral interstitial nucleus of the medial longitudinal fasciculus. *Exp. Brain Res.* 106: 215–232, 1995.

SUZUKI, Y., STRAUMANN, D., HESS, B.J.M., AND HENN, V. Changes of Listing's plane under physiological and pathological conditions. In: *Information Processing Underlying Gaze Control,* edited by J. M. Delgado-Garcia, E. Godaux, and P. P. Vidal. Oxford: Pergamon, 1994, p. 75–86.

TWEED, D., FETTER, M., ANDREADAKI, S., KOENIG, E., AND DICHGANS, J. Three-dimensional properties of human pursuit eye movements. *Vision Res.* 32: 1225–1238, 1992.

TWEED, D. AND VILIS, T. Implications of rotational kinematics for the oculomotor system in three dimensions. *J. Neurophysiol.* 58: 832–849, 1987.

TWEED, D. AND VILIS, T. Geometric relations of eye position and velocity vectors during saccades. *Vision Res.* 30: 111–127, 1990.

VAN DEN BERG, A. V. Kinematics of eye movement control. *Proc. R. Soc. Lond. B Biol. Sci.* 260: 191–197, 1995.

VAN OPSTAL, A. J., HEPP, K., SUZUKI, Y., AND HENN, V. Role of monkey nucleus reticularis tegmenti pontis in the stabilization of Listing's plane. *J. Neurosci.* 16: 7284–7296, 1996.

VAN RIJN, L. J., VAN DER STEEN, J., AND COLLEWIJN, H. Instability of ocular torsion during fixation: cyclovergence is more stable than cycloversion. *Vision Res.* 34: 1077–1087, 1994.

ZEE, D. S., YAMAZAKI, A., BUTLER, P. H., AND GUCER, G. Effects of ablation of flocculus and paraflocculus of eye movements in primate. *J. Neurophysiol.* 46: 878–899, 1981.